Nuclear Instruments and Methods in Physics Research A 620 (2010) 270–278

Contents lists available at ScienceDirect

Nuclear Instruments and Methods in Physics Research A

journal homepage: www.elsevier.com/locate/nima

Characterization of charge carrier collection in a CdZnTe Frisch collar detector with a highly collimated ^{137}Cs source

Alireza Kargar [a], Mark J. Harrison [b], Adam C. Brooks [a], Douglas S. McGregor [a,*]

[a] S.M.A.R.T. Laboratory, Department of Mechanical and Nuclear Engineering, Kansas State University, Manhattan, KS 66506, USA
[b] Nuclear and Radiological Engineering, University of Florida, 202 NSB, Gainesville, FL 32611, USA

ARTICLE INFO

Article history:
Received 7 July 2009
Received in revised form
1 February 2010
Accepted 16 February 2010
Available online 20 February 2010

Keywords:
Room temperature semiconductor spectrometers
CdZnTe spectrometer
Frisch collar detector

ABSTRACT

A 4.7 × 4.7 × 9.5 mm^3 CdZnTe Frisch collar device was characterized through probing the device with a highly collimated ^{137}Cs 662 keV gamma ray source. In a systematic series of experiments, the detector was probed along the length and width with a ^{137}Cs gamma ray source using a 43.0 mm long Pb-collimator with a 0.6 mm circular hole. The detector was probed along the central line under different operating voltages of 1200, 1000, 800, 600 and 400 V. The experimental results correlated well to charge collection calculations for a modeled device with the same size and operating conditions. It was proved that, unlike the planar configuration, the charge collection efficiency profile along the length of Frisch collar device is considerably improved. The CdZnTe raw materials for this study were acquired from Redlen Technologies, and the Frisch collar device was fabricated and characterized at S.M.A.R.T. Laboratory at Kansas State University.

1. Introduction

An ideal gamma ray spectrometer would operate at room temperature, exhibit low noise characteristics, possess good gamma ray absorption efficiency, and have high energy resolution. The relatively wide band gap and high resistivity of CdZnTe, along with its high effective Z-number (which provides good gamma ray absorption efficiency), allows CdZnTe to be a good candidate for room-temperature operated gamma-ray spectrometers. CdZnTe Frisch collar detectors demonstrate promising results as high energy resolution gamma-ray spectrometers [1–4], which perform as single carrier devices by negating the deleterious effects of hole trapping [1–16]. Further, the simplicity of the Frisch collar device lowers manufacturing costs and makes it attractive as a portable instrument.

An important gamma-ray spectrometer characteristic is the uniformity of response to gamma ray interactions. In other words, it is important that the pulse height response is constant for any given energy deposited in the detector and is not dependent upon the location where the gamma ray was absorbed. For a device with large differences in charge carrier trapping times between electrons and holes, a *non-uniform* current induction distribution along the device length can reduce position dependent responses and allows for enhanced energy resolution [9].

The charge collection distribution for a Frisch-collar type device was first reported for a trapezoidal-shaped Frisch grid CdZnTe gamma-ray detector [11]. In a systematic series of experiments, the detector was probed with a collimated ^{241}Am 59.5 keV gamma-ray source along the bottom cathode and the sides. For cathode and sidewall probing, almost all charge carriers were excited near the surface because 97% of 59.5 keV gamma rays are absorbed within 1.0 mm of CdZnTe material surface. The results of the study proved that the charge-carriers were collected uniformly from all locations along the surface. A similar study was later conducted along the length of a bar-shaped Frisch collar device using a collimated gamma-ray source [16]. The study was performed for a 3.4 × 3.4 × 5.5 mm^3 CdZnTe Frisch collar device, with a variety of conductive Frish collar lengths [16]. It was shown that the charge collection efficiency (CCE) profile along the length of a Frisch collar detector is considerably improved over that of a planar detector. The study clearly showed and confirms the robustness of Frisch collar technology.

In this study, CCE characterization of a two terminal 4.7 × 4.7 × 9.5 mm^3 CdZnTe Frisch collar device is performed by probing the Frisch collar device with highly collimated ^{137}Cs gamma ray source. The collimator was a 43.0 × 43.0 × 43.0 mm^3 lead block with a 0.6 mm diameter hole through a central axis. The collimator was fabricated by pouring molten lead into a cast with a 0.6 mm diameter steel rod placed vertically in the center of the cast. After the lead cooled, the steel rod was removed, leaving behind the collimator hole. The spectroscopic response was investigated by probing the entire lateral side of the CdZnTe Frisch collar device with the collimated ^{137}Cs gamma ray source.

* Corresponding author.
E-mail address: mcgregor@ksu.edu (D.S. McGregor).
URL: http://www.mne.ksu.edu/research/centers/SMARTlab (D.S. McGregor).

0168-9002/$ - see front matter © 2010 Elsevier B.V. All rights reserved.
doi:10.1016/j.nima.2010.02.104

The experimental results correlated well to charge collection efficiency models for detectors with the same dimensions and operating conditions.

2. Theoretical considerations

The CdZnTe Frisch collar device used in this study was operated with the conductive collar grounded and the collecting contact positively biased. Laplace's equation is used to determine the position dependent current induction from the *weighting potential* distribution V_w [17],

$$\nabla(\kappa\varepsilon_0\nabla V_w)=0 \tag{1}$$

where ε_0 is the permittivity of vacuum and κ is the material dielectric constant. The weighting potential $V_w(x,y,z)$ distribution is normalized, in which the collecting electrode (anode in this case) is set to unity (V_w = 1) with all other electrodes grounded (V_w = 0). If more than one media exists within the domain, then Laplace's equation must to be solved separately in each medium with appropriate κ values and appropriate boundary conditions. The *weighting field* distribution E_w (cm^{-1}) is determined with [17],

$$E_w(x,y,z)=-\nabla V_w. \tag{2}$$

Poisson's equation is used to determine the *operating potential* V, which is the actual voltage distribution within the detector during operation,

$$\nabla(\kappa\varepsilon_0\nabla V)=-\rho \tag{3}$$

where ρ is the space charge density. With the absence of space charge, Poisson's equation reduces to Laplace's equation, and the operating potential and electric field for a two terminal device become,

$$V(x,y,z)=\Delta V\cdot V_w(x,y,z) \tag{4}$$

and,

$$E(x,y,z)=\Delta V\cdot E_w(x,y,z) \tag{5}$$

where ΔV is the voltage drop across the detector contacts. Under the special operating condition that the collecting electrode is biased and the non-collecting electrode is grounded, the operating potential and electric field for a *two-terminal* Frisch collar device reduce to,

$$V(x,y,z)=H_V\cdot V_w(x,y,z) \tag{6}$$

and,

$$E(x,y,z)=H_V\cdot E_w(x,y,z) \tag{7}$$

where H_V is the high voltage applied to the detector, $V(x,y,z)$ is the operating potential distribution in volts, and $E(x,y,z)$ is the electric field distribution in V cm^{-1}. Therefore, the voltage distribution $V(x,y,z)$ resembles the distribution of the weighting potential $V_w(x,y,z)$, scaled by H_V. Similarly, the electric field distribution $E(x,y,z)$ resembles the weighting field distribution $E_w(x,y,z)$ for a two-terminal device also scaled by H_V.

By applying the Shockley–Ramo theorem [18,19], an analysis method initially applied to vacuum tubes, but later shown to be valid for semiconductor detector analysis [17,20–24,26], CCE maps for a Frisch collar device can be determined. It is assumed that the effect of recombination and long term trapping of the charge carriers is well-represented by a single value, the mean free drift time τ, while considering de-trapping effects negligible [25]. The mean free drift time is used to determine the average time interval in which current is induced on the desired electrode before a charge carrier is lost. The time needed to collect a charge carrier type (either electrons or holes) from any random starting location in the detector to its corresponding electrode is denoted t_c, and is dependent upon the mobility and electric field.

For the following analysis, the authors draw attention to the coordinate convention shown in Fig. 1. Consider the case in which a gamma ray interacts in a radiation detector and N_0 charge pairs are excited at time t = t_0 = 0 at a random location x_0. A voltage applied across the device will cause electrons to drift towards the anode and the holes to drift towards the cathode. The total number of free charge carriers $N(t)$ remaining in motion at time $t=t'$ is,

$$N(t)=N_0\exp\left[-\frac{t'}{\tau_e}\right]+N_0\exp\left[-\frac{t'}{\tau_h}\right] \tag{8}$$

where τ_e and τ_h are the mean free drift times for electrons and holes, respectively. For simplicity, it is assumed that charge carriers have a velocity related to the charge carrier mobility μ and electric field,

$$v(x)=\frac{dx}{dt}=\mu E(x). \tag{9}$$

Hence, for any segment of time past t_0,

$$t'=\frac{x}{v}=\frac{x}{\mu E(x)} \tag{10}$$

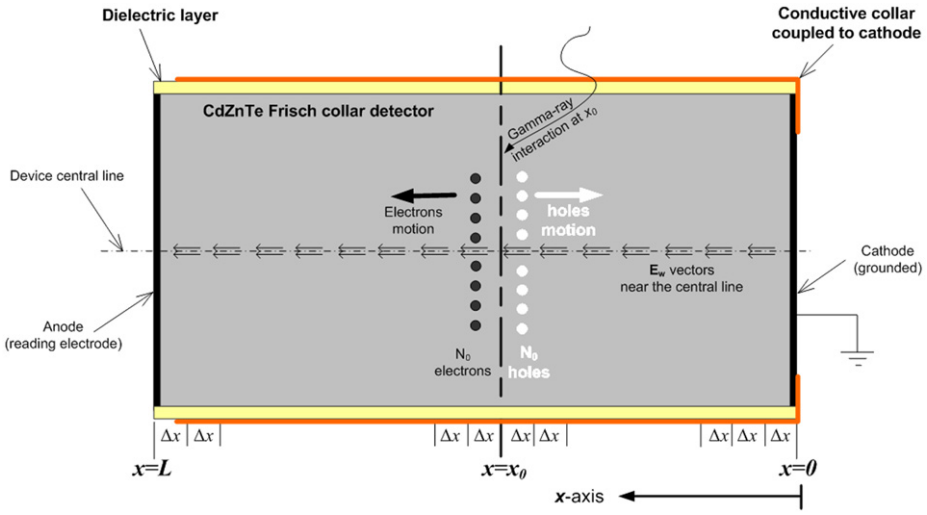

Fig. 1. Coordinate system for the Frisch collar device under investigation. Notice that the positive x direction increases towards the left.

where x is the distance traveled. Consider a device of total length L where an ionizing event has occurred at location x_0. Assume the convention where electrons move in the positive 'x' direction and holes move in the negative 'x' direction. Substituting Eq. (10) into Eq. (8), the remaining number of charge carriers is

$$N(t) = N_0 \exp\left[\frac{x_0 - x_e}{\mu\tau_e E(x)}\right] + N_0 \exp\left[\frac{x_h - x_0}{\mu\tau_h E(x)}\right] \tag{11}$$

where x_e is the position of the electron cloud and x_h is the position of the hole cloud. Note that the actual charge in motion is

$$Q(t) = -qN_0 \exp\left[\frac{x_0 - x_e}{\mu\tau_e E(x)}\right] - qN_0 \exp\left[\frac{x_h - x_0}{\mu\tau_h E(x)}\right]. \tag{12}$$

As the charge carriers move through the device and experience trapping, the differential change in the induced charge at the device terminals is a function of the total number of charges in motion and the differential weighting potential through which they move,

$$dQ(t) = -qN_0 \exp\left[\frac{x_0 - x_e}{\mu\tau_e E(x)}\right] dV_w\Big|_{x_e} - qN_0 \exp\left[\frac{x_h - x_0}{\mu\tau_h E(x)}\right] dV_w\Big|_{x_h}. \tag{13}$$

For a differential change in charge carrier location, the weighting potential can be described as

$$dV_w = E_w\, dx \tag{14}$$

where E_w is the weighting field at either x_e or x_h (depending on the evaluation point), and Eq. (13) becomes,

$$dQ(t) = -Q_0 E_w(x_e) \exp\left[\frac{x_0 - x_e}{\mu\tau_e E(x)}\right] dx\Big|_{x_e} - Q_0 E_w(x_h) \exp\left[\frac{x_h - x_0}{\mu\tau_h E(x)}\right] dx\Big|_{x_h}. \tag{15}$$

The total change in the induced charge can be determined by integrating the induced charge dQ over the length of the Frisch collar device. It is this *change* in the induced charge, that is measured by electronic spectroscopy circuits, often simply referred to as the *induced current*. The induced current can be stored on an external capacitor, commonly referred to as the *induced charge*.

A close estimate of the same operation can be performed by summing the incremental induced charge ΔQ for each incremental change in position Δx over the entire device. Take, for instance, a Frisch collar detector that has been divided into N segments labeled as Δx. Here, one can write,

$$\Delta x = \frac{L}{N} \tag{16}$$

where L is the length of the Frisch collar device. The number of remaining free charge carriers at time t_i after the initial event at time t_0 is described by

$$Q_i(t_i) = Q_0 \exp\left[\frac{t_0 - t_i}{\tau_e}\right] + Q_0 \exp\left[\frac{t_0 - t_i}{\tau_h}\right] \tag{17}$$

provided that $t_i \le t_c$ of either charge carrier. For the special case in which charges are moving along the central longitudinal axis of the device, it can be assumed that the change in induced charge is dependent upon charges moving parallel along the axis, designated as the x direction in the present case. It is also assumed that charge cloud diffusion is negligible compared to charge cloud drift. This assumption is valid for detectors with large area

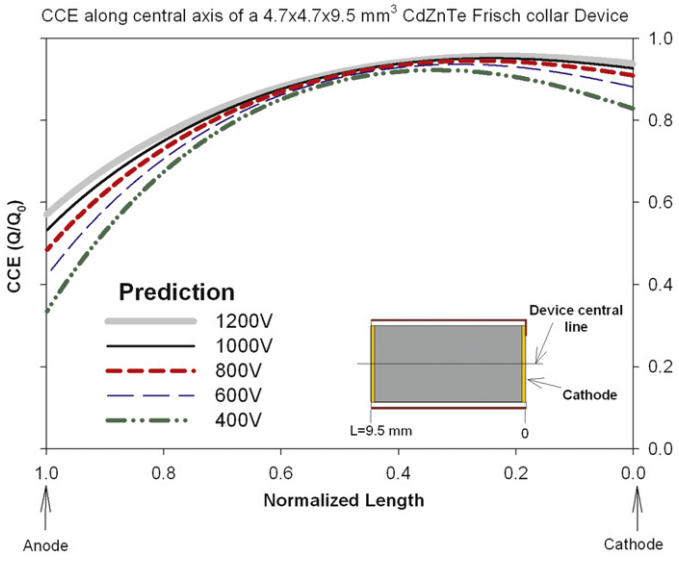

Fig. 2. The charge collection efficiency (CCE) profile at different voltages of 1200, 1000, 800, 600 and 400 V applied to anode (collecting electrode) along the central line of a $4.7 \times 4.7 \times 9.5\,mm^3$ CdZnTe Frisch collar device. The CCE is plotted based on Shockley–Ramo theorem and through electric field and weighting field modeling of the device with 0.35 mm of insulator layer, and 9.5 mm long Frisch collar (entire device) held at cathode bias (grounded).

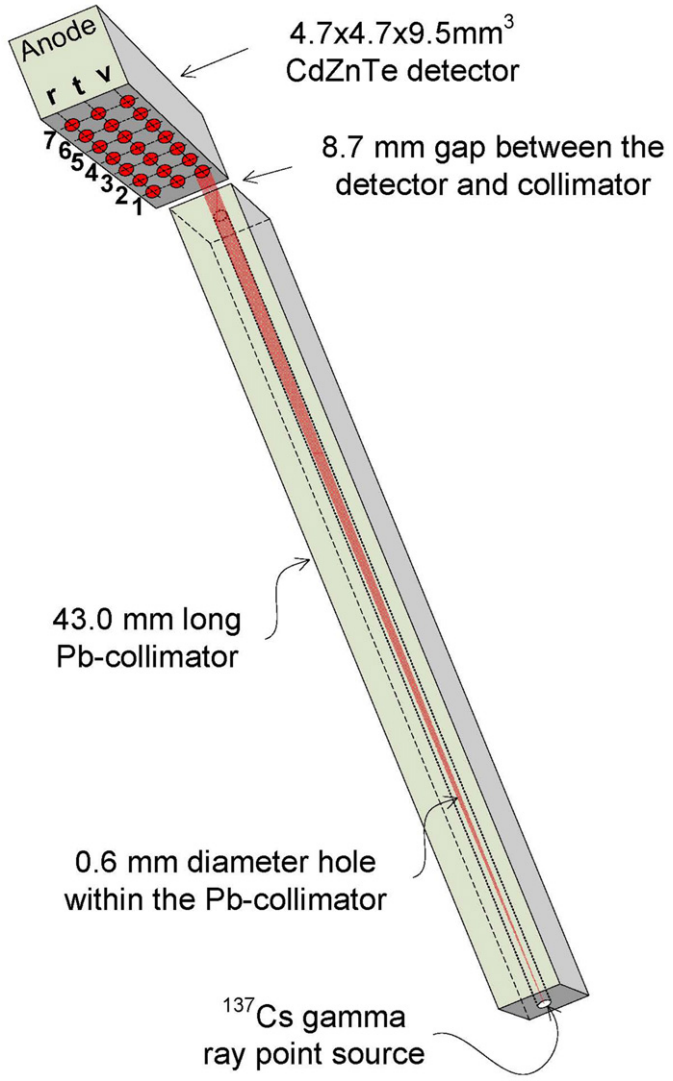

Fig. 3. The schematic setup for the gamma ray source, Pb-collimator, and the CdZnTe Frisch collar detector, showing only the narrow collimater hole section of the $43.0 \times 43.0 \times 43.0\,mm^3$ Pb-collimator. A 2MBq ^{137}Cs gamma ray source was placed at the far end of 0.6 mm circular hole. The CdZnTe Frisch collar detector was held stationary at a distance of 8.7 mm from the emerging end of the Pb-collimator. The $43.0 \times 43.0 \times 43.0\,mm^3$ Pb-collimator block and gamma ray source were mounted on a linear stage with two degrees of freedom, and adjusted to irradiate specific probing locations along the Frisch collar detector.

collecting electrodes, such as Frisch collar detectors with electrode surface areas of $4.7 \times 4.7\,mm^2$. Diffusion effects can, however, contribute significantly for long drift detectors with small collection areas, such as observed with pixelated devices [6].

The transport time intervals $\Delta t_{e,h}$ over incremental distances of Δx for electrons and holes are

$$\Delta t_{e,h} = \frac{\Delta x}{v_{e,h}} = \frac{\Delta x}{\mu_{e,h} E} \tag{18}$$

where $v_{e,h}$ is the velocity (cm s^{-1}) of either the electrons or holes; and E is magnitude of electric field (V cm^{-1}) in the direction of charge carrier motion. From any starting location x_0, holes will travel from $x = x_0$ to 0 and electrons travel from x_0 to L. Dividing the device into N segments, the electron contribution to the change in the induced charge at location x_i after moving from location x_{i-1} is

$$\Delta Q_i(t_i) = Q_{i-1} \Delta V_w(x_i) \exp\left[\frac{-\Delta x}{\mu \tau_e E(x_i)}\right] \tag{19}$$

$$= Q_{i-1} E_w(x_i) \exp\left[\frac{-\Delta x}{\mu \tau_h E(x_i)}\right] \Delta x \tag{20}$$

and the hole contribution to the change in the induced charge at location x_j after moving from location x_{j-1} is

$$\Delta Q_j(t_j) = Q_{j-1} \Delta V_w(x_j) \exp\left[\frac{-\Delta x}{\mu \tau_e E(x_j)}\right] \tag{21}$$

$$= Q_{j-1} E_w(x_j) \exp\left[\frac{-\Delta x}{\mu \tau_h E(x_j)}\right] \Delta x \tag{22}$$

where $E(x)$ (V cm^{-1}) is the actual electric field at the charge carrier location, and the terms E_w and ΔV_w are the normalized weighting field and the change in the normalized weighting

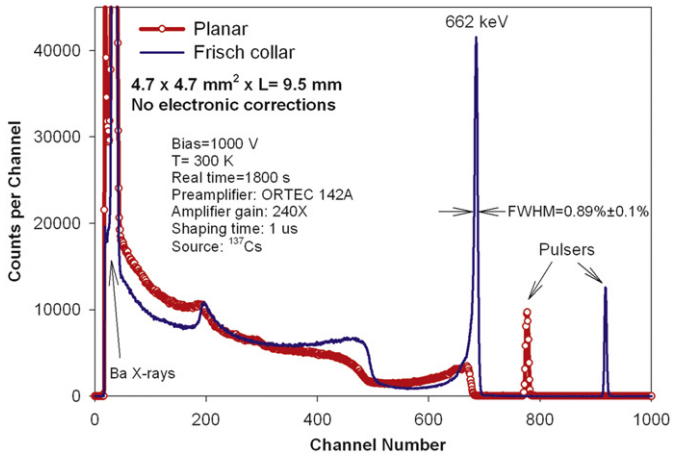

Fig. 4. Pulse height spectra taken with the $4.7 \times 4.7 \times 9.5\,mm^3$ CdZnTe Frisch collar device being fully radiated with a ^{137}Cs gamma ray source positioned right underneath the device. The measurement setup and equipment are listed on the figure. A 0.89% FWHM energy resolution is achieved at 662 keV.

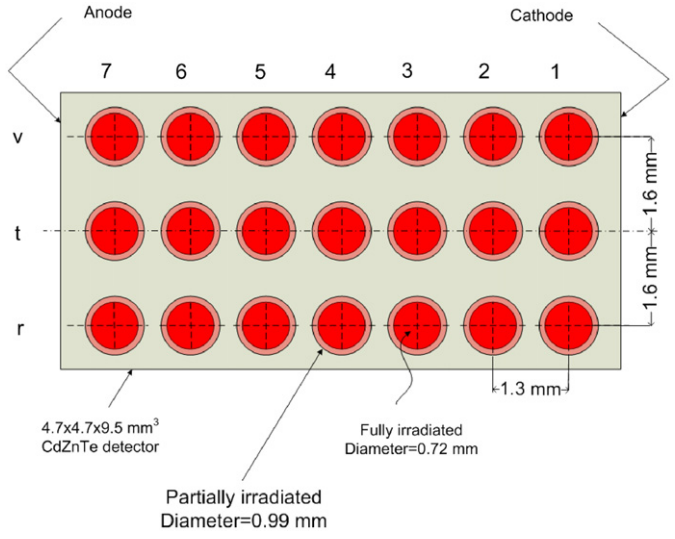

Fig. 5. The irradiated points on the $4.7 \times 4.7 \times 9.5\,mm^3$ CdZnTe Frisch collar device. The collimated gamma ray source on a linear stage allows for irradiating the desired points shown on the CdZnTe device. The Frisch collar device was radiated in increments of 1.3 mm along the length, and 1.6 mm along the width. The partially irradiated area is due to the size of the ^{137}Cs gamma ray source, which was comparable to the collimator hole (0.6 mm).

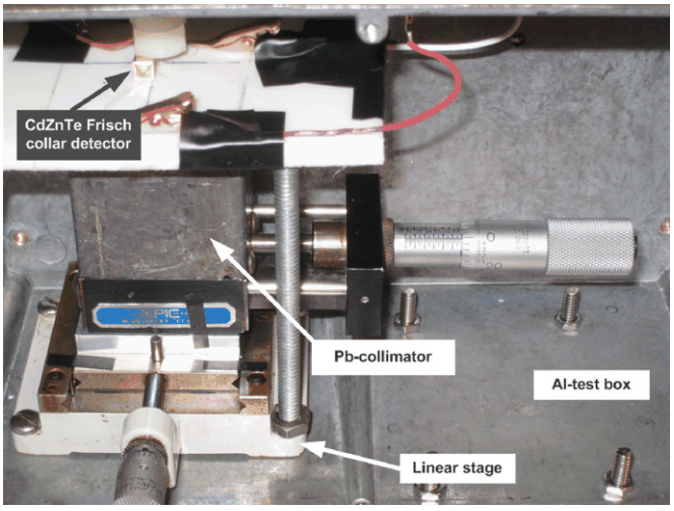

Fig. 6. The Pb collimator/detector arrangement within the Al test box. The Pb collimator is mounted on a linear stage with two degrees of freedom, and the CdZnTe Frisch collar detector is stationary, ready to be probed by the collimated gamma ray source.

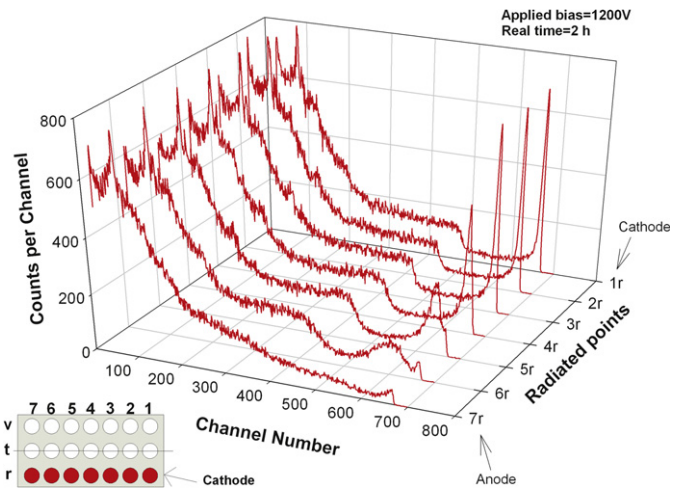

Fig. 7. Pulse height spectra collected from a collimated ^{137}Cs gamma ray source with the $4.7 \times 4.7 \times 9.5\,mm^3$ CdZnTe Frisch collar device. The Frisch collar device was probed with a highly collimated gamma ray source along row r at 1200 V for 2 h real time.

potential, respectively, over distance Δx. The $\mu_e\tau_e$ and $\mu_h\tau_h$ are assumed to be constant over the entire device.

For equal incremental distances Δx, the total measured induced charge ΔQ_T is the summation of the charge induced per segment by the electrons traveling from point x_0 to the anode (from $x = x_0$ to $x = L$) and the charge induced per segment by the holes traveling from point x_0 to the cathode (from $x = x_0$ to $x = 0$),

$$\Delta Q_T = -\sum_{i=x_0}^{L} \Delta Q_i \Big|_e - \sum_{j=0}^{x_0} \Delta Q_j \Big|_h \tag{23}$$

noting that appropriate signs are needed for charge carrier direction and charge carrier type (negative or positive). The charge collection efficiency CCE(x_0) for a gamma-ray interaction at location x_0 can be evaluated as

$$CCE(x_0) = \frac{\sum_{i=x_0}^{L} \Delta Q_i \Big|_e + \sum_{j=0}^{x_0} \Delta Q_j \Big|_h}{Q_0} = -\frac{\Delta Q_T}{Q_0}. \tag{24}$$

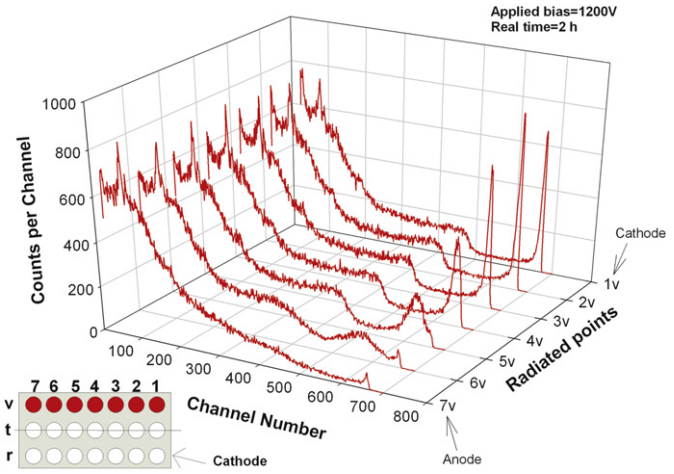

Fig. 8. Pulse height spectra collected from a collimated ^{137}Cs gamma ray source with the $4.7 \times 4.7 \times 9.5\,mm^3$ CdZnTe Frisch collar device. The Frisch collar device was probed with a highly collimated gamma ray source along row *v* at 1200 V for 2 h real time. Note that there is a beveled corner at top right part of the device near the cathode (row *v*, column 1), which accounts for the lower number of counts in the spectrum at 1 *v* in the graph.

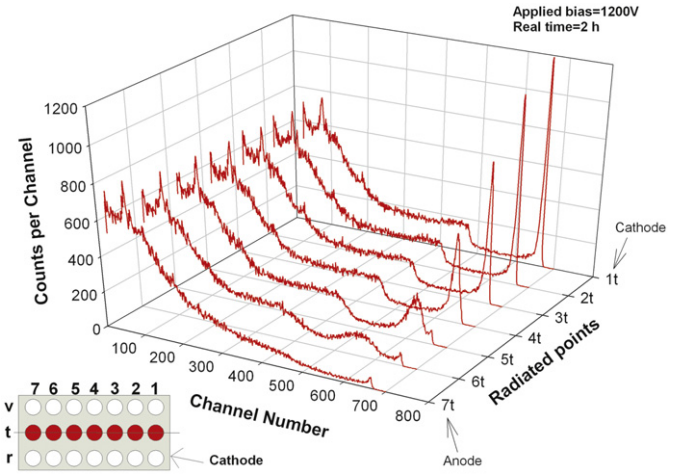

Fig. 9. Pulse height spectra collected from a collimated ^{137}Cs gamma ray source with the $4.7 \times 4.7 \times 9.5\,mm^3$ CdZnTe Frisch collar device. The Frisch collar device was probed with a highly collimated gamma ray source along row *t* at 1200 V for 2 h real time.

Plots of *CCE* for a two-terminal $4.7 \times 4.7 \times 9.5\,mm^3$ CdZnTe Frisch collar device at different applied voltage (H_V) are provided in Fig. 2. The plots are along the device central line where the electric field (and weighting field) vectors lay on a straight line. The device length L is divided into 1000 segments of Δx for the numerical simulation. The device is modeled in three-dimensional geometry, and the weighting field and electric field distributions were determined using Integrated Engineering Software, LORENTZ. The mobility-lifetime products of 0.045 and 10^{-4} cm^2 V^{-1} were assumed for the electrons and holes, respectively.

3. Experimental procedure

A $4.7 \times 4.7 \times 9.5\,mm^3$ CdZnTe Frisch collar device was fabricated as previously reported [5]. The CdZnTe raw materials for this study were acquired from Redlen Technologies. The collimator was formed from a cast $43 \times 43 \times 43\,mm^3$ Pb block with a 0.6 mm circular hole formed clear through perpendicular to one of

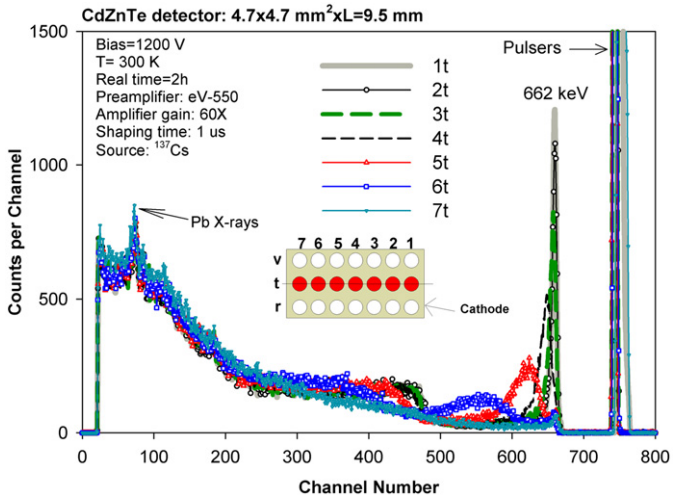

Fig. 10. Pulse height spectra collected from a collimated ^{137}Cs gamma ray source with the $4.7 \times 4.7 \times 9.5\,mm^3$ CdZnTe Frisch collar device. The Frisch collar device was probed with a highly collimated gamma ray source along row *t* at 1200 V for 2 h real time. The measurement setup and equipment are listed on the figure.

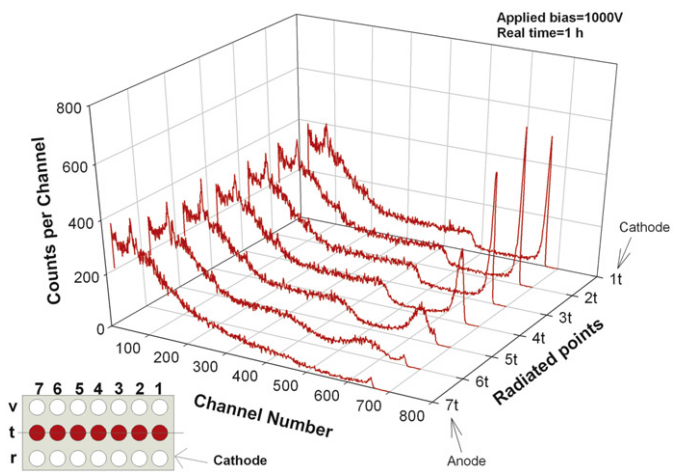

Fig. 11. Pulse height spectra collected from a collimated ^{137}Cs gamma ray source with the $4.7 \times 4.7 \times 9.5\,mm^3$ CdZnTe Frisch collar device. The Frisch collar device was probed with a highly collimated gamma ray source along row *t* at 1000 V for 1 h real time.

the faces. The 43.0 mm Pb thickness attenuates approximately 99.6% of 662 keV gamma rays, and the large block of material reduces Compton scattered gamma rays from entering the CdZnTe detector. Due to beam divergence through the collimator, the irradiated region at the surface of the CdZnTe detector was a 0.72 mm diameter circle. The collimator-detector geometry and the irradiated points on CdZnTe Frisch collar detector are depicted in Fig. 3.

Before performing the probing experiment, pulse height spectra were taken using a ^{137}Cs gamma ray source placed directly below the fabricated CdZnTe device, first in the planar configuration and afterwards in the Frisch collar configuration. Comparison pulse height spectra for the entire device being irradiated with 662 keV gamma rays are shown in Fig. 4. Sub-0.9% full width half maximum (FWHM) energy resolution at 662 keV is achieved for the Frisch collar device with no electronic correction while using a commercial ORTEC 142A preamplifier. The measurement settings and the counting time are shown in Fig. 4.

The Pb-collimator was mounted on a linear stage with two degrees of freedom, allowing the $4.7 \times 4.7 \times 9.5\,mm^3$ CdZnTe Frisch collar device to be probed by the highly collimated ^{137}Cs gamma ray source at desired locations along the length and width of the device (see Fig. 5). The irradiation matrix has 21 locations with seven x-coordinate positions and three y-coordinate positions, labeled (r, t and v). The Frisch collar detector was placed 8.7 mm away from the Pb-collimator and was held stationary during all measurements (Fig. 6). The ^{137}Cs gamma ray source was placed on the linear stage and aligned underneath the Pb collimator hole. The detector, gamma ray source, Pb-collimator and the linear stage were placed inside an aluminum test box, as shown in Fig. 6.

The $4.7 \times 4.7 \times 9.5\,mm^3$ CdZnTe Frisch collar device was then probed with the collimated ^{137}Cs gamma ray source to investigate the uniformity of the Frisch collar device's response to 662 keV gamma rays. The aluminum test box was connected to an eV-550 preamplifier through an SHV connector. The aluminum test box and preamplifier were placed inside a copper Faraday cage. The

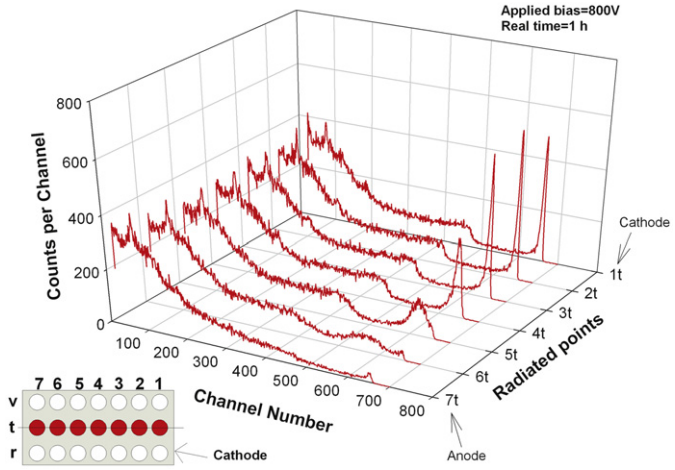

Fig. 12. Pulse height spectra collected from a collimated ^{137}Cs gamma ray source with the $4.7 \times 4.7 \times 9.5\,mm^3$ CdZnTe Frisch collar device. The Frisch collar device was probed with a highly collimated gamma ray source along row t at 800 V for 1 h real time.

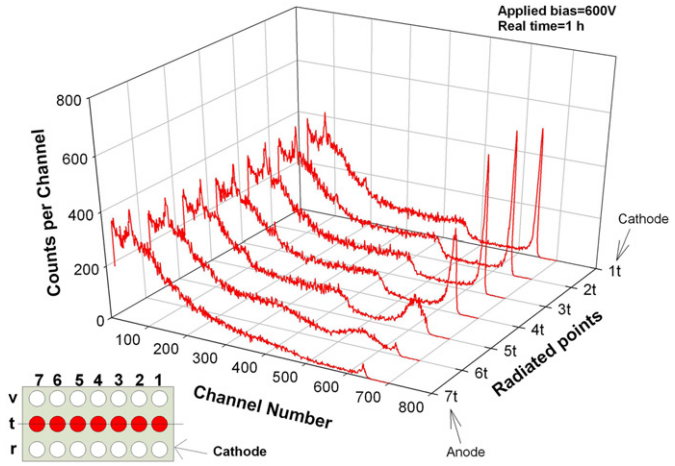

Fig. 13. Pulse height spectra collected from a collimated ^{137}Cs gamma ray source with the $4.7 \times 4.7 \times 9.5\,mm^3$ CdZnTe Frisch collar device. The Frisch collar device was probed with a highly collimated gamma ray source along row t at 600 V for 1 h real time.

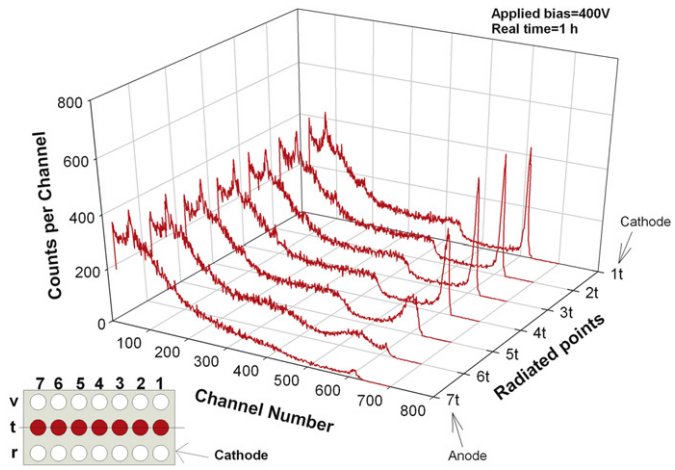

Fig. 14. Pulse height spectra collected from a collimated ^{137}Cs gamma ray source with the $4.7 \times 4.7 \times 9.5\,mm^3$ CdZnTe Frisch collar device. The Frisch collar device was probed with a highly collimated gamma ray source along row t at 400 V for 1 h real time.

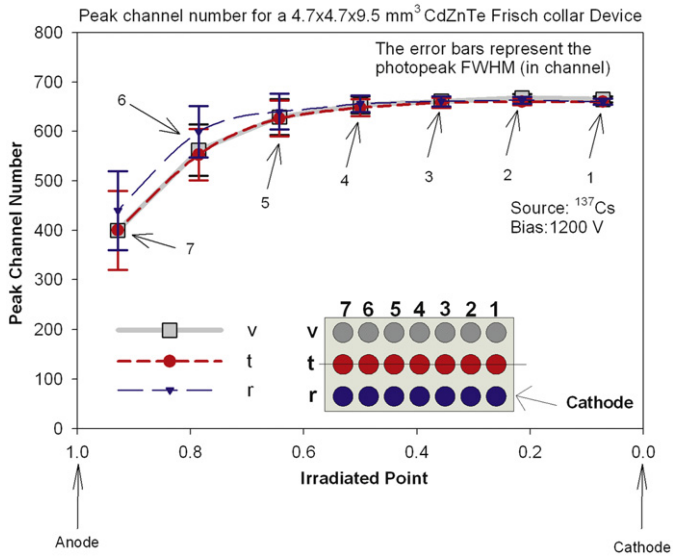

Fig. 15. The peak channel of photo-peak for the irradiated points of the $4.7 \times 4.7 \times 9.5\,mm^3$ CdZnTe Frisch collar device. The Frisch collar device was probed with a highly collimated gamma ray source of ^{137}Cs along row r, row t (central line) and row v at 1200V. The error bars are representing the photo-peak FWHM in channel and are shown for all the data points.

preamplifier was connected to a high-voltage supply, amplifier (CANBERRA Model 2021) and a pulse generator. An oscilloscope, a multichannel analyzer (MCA) and a personal computer were used to monitor and acquire the data. At an operating bias of 1200 V, the device lateral side was probed at the indexed positions shown in Fig. 5, where a 2 h radiation measurement was conducted for each of the twenty one probe locations. The pulse height spectra acquired for the twenty one data points are presented in Figs. 7–10.

Afterwards, the device was probed along the central axis for all positions on row t at operating bias voltages of 1000, 800, 600, and 400 V. For the different bias voltages, 1 h real time radiation measurements were conducted for each of the seven probe locations of row t. Accurate source placement was performed by moving the collimator-source with the two-dimensional linear stage in increments of 1.3 mm along the device central line (row t at locations 1–7 in Fig. 5). The pulse height spectra are presented in Figs. 11–14.

4. Results and discussions

The spectra collected (Figs. 7–14) from the CdZnTe Frisch collar device as irradiated with the collimated ^{137}Cs gamma ray source shows a uniform response for most of the device volume. This uniform response to gamma rays is confirmed after plotting the

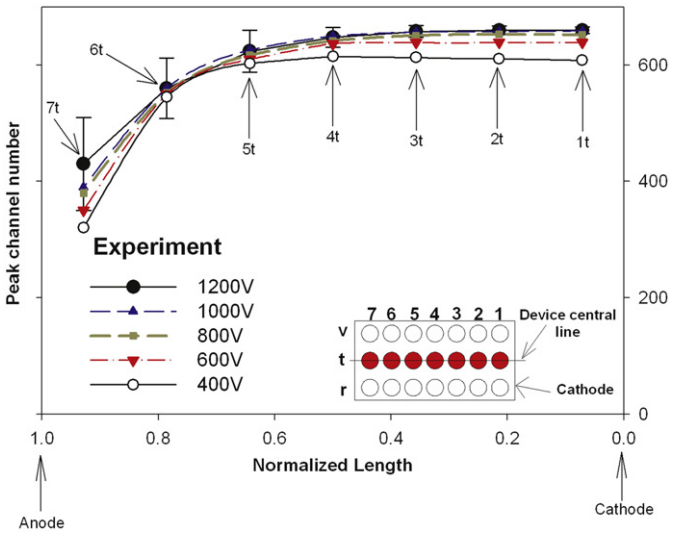

Fig. 16. The peak channel of photo-peak for the irradiated points of the $4.7 \times 4.7 \times 9.5\ mm^3$ CdZnTe Frisch collar device. The Frisch collar device was probed with a highly collimated gamma ray source of ^{137}Cs along row t (central line) at different voltages of 1200 V, 1000 V, 800 V, 600 V and 400 V applied to anode (collecting electrode). The error bars are representing the photo-peak FWHM in channel and are shown only for the data points collected at 1200V.

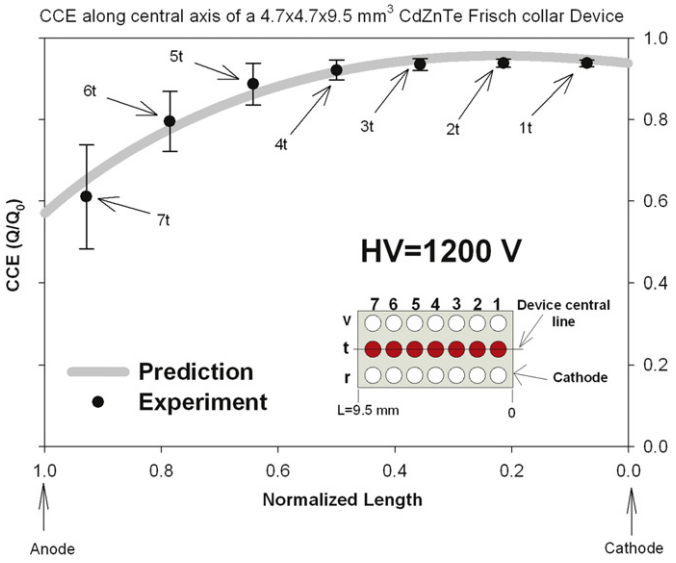

Fig. 17. The CCE profile at 1200 V applied to anode (collecting electrode) along the central line of the $4.7 \times 4.7 \times 9.5\ mm^3$ CdZnTe Frisch collar device. The experimental data points are the normalized peak channel of photo-peak for the irradiated points (row t) of the Frisch collar device. The error bars represent the photo-peak FWHM.

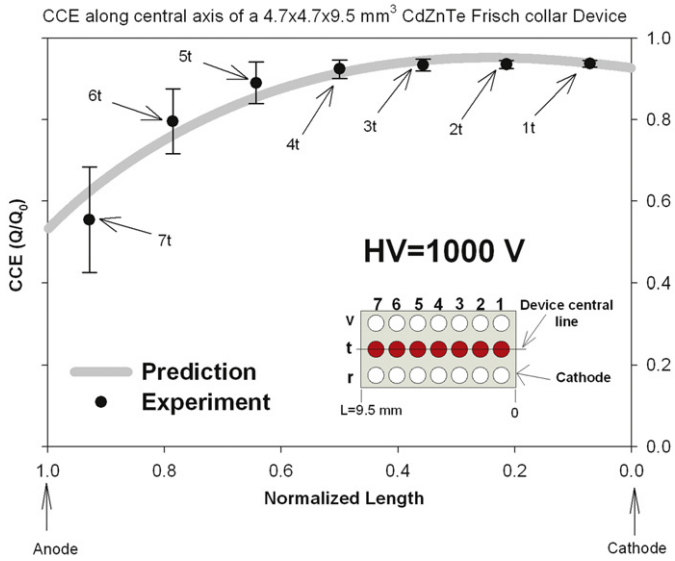

Fig. 18. The CCE profile at 1000 V applied to anode (collecting electrode) along the central line of the $4.7 \times 4.7 \times 9.5\ mm^3$ CdZnTe Frisch collar device. The experimental data points are the normalized peak channel of full energy peak for the irradiated points (row t) of the Frisch collar device. The error bars represent the full energy peak FWHM.

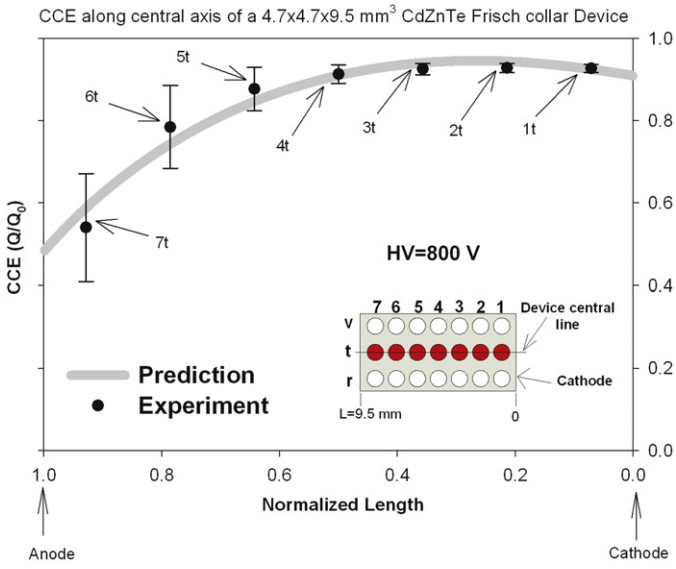

Fig. 19. The CCE profile at 800 V applied to anode (collecting electrode) along the central line of the $4.7 \times 4.7 \times 9.5\ mm^3$ CdZnTe Frisch collar device. The experimental data points are the normalized peak channel of full energy peak for the irradiated points (row t) of the Frisch collar device. The error bars represent the full energy peak FWHM.

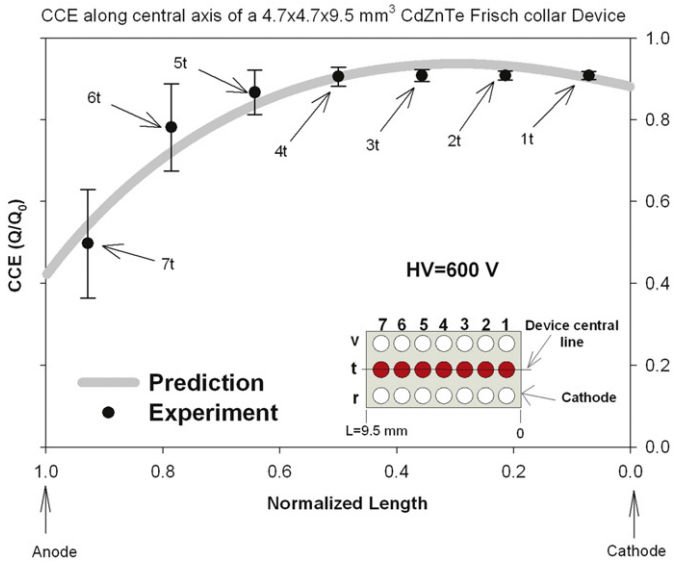

Fig. 20. The CCE profile at 600 V applied to anode (collecting electrode) along the central line of the $4.7 \times 4.7 \times 9.5\,mm^3$ CdZnTe Frisch collar device. The experimental data points are the normalized peak channel of full energy peak for the irradiated points (row t) of the Frisch collar device. The error bars represent the full energy peak FWHM.

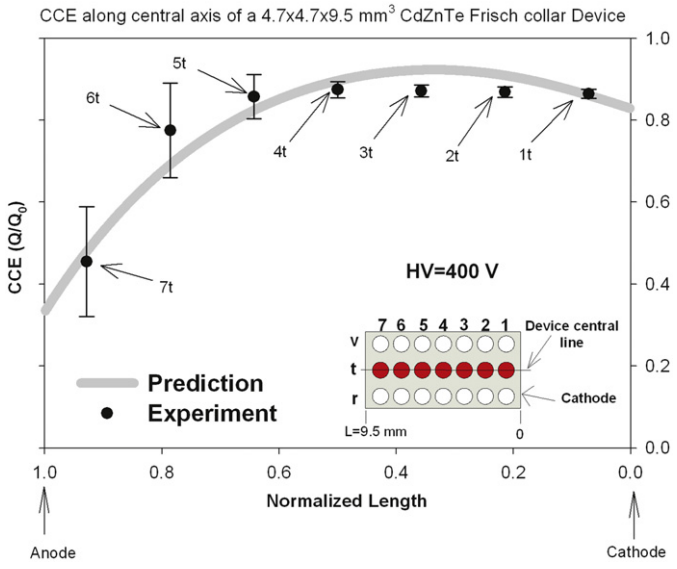

Fig. 21. The CCE profile at 400 V applied to anode (collecting electrode) along the central line of the $4.7 \times 4.7 \times 9.5\,mm^3$ CdZnTe Frisch collar device. The experimental data points are the normalized peak channel of full energy peak for the irradiated points (row t) of the Frisch collar device. The error bars represent the full energy peak FWHM.

peak channel number of each spectrum versus the irradiated positions, as shown in Figs. 15 and 16. From Fig. 15, the peak channel of the full energy peak remained unchanged for nearly two-thirds of the device length (from columns 1 to 5) and for the entire device width (rows r, t and v). The peak channel location is consistent for spectra collected along rows r, t and v (Figs. 7–9).

The full energy peak channel for spectra along the device central line (row t) at different applied voltages is presented in Fig. 16. The peak channel of the full energy peak remained unchanged for approximately two-thirds of the device (from columns 1 to 5) even at the low applied voltage of 400 V. This characteristic response is also observed from the spectra presented in Figs. 9–14. The experimental results of Fig. 16 and the theoretical predictions of Fig. 2 compare well. Comparisons for each bias voltage increment are shown in Figs. 17–21. Notice in all cases the experimental results match well with the theoretical prediction, clearly showing that the Frisch collar device responds uniformly to gamma rays over most of the detector volume. This uniform response is observed despite the non-uniform electric field distribution within the device and the relatively low electric field near the cathode region [27]. Even though the electric field distribution is relatively low near the cathode region, the device performance is actually enhanced in that region. In other words, the overall energy resolution enhancement on device spectral performance is so remarkable that sub-0.9% FWHM energy resolution is achieved without any electronic correction (Fig. 6).

Finally, there is a feature present in all spectra (Figs. 7–14), a small peak, that appears for irradiated data points near the anode (columns 5, 6 and 7). The feature appears due to the uncollided 662 keV gamma rays, which pass unattenuated through the lead collimator edges and interact in regions of the device outside the probed area. These low flux uncollided 662 keV gamma rays interact in other regions of device with better CCE (regions between columns 1 and 5), thereby producing a tiny peak in the full energy channel, clearly seen as a new feature in column 6 of all spectra (Figs. 7–14).

Note that the Frisch collar detector, as a single carrier device, is a robust design that achieves sub-0.9% FWHM energy resolution without any digital or electronic corrections. Unlike many other single carrier device designs, such as pixelated devices [28] and co-planar devices [29], the Frisch collar device does not need electronic corrections to produce sub-1% FWHM energy resolution. Comparing the uncorrected spectra of three reported single carrier designs (Frisch collar device in Fig. 6, pixelated device [28], and co-planar device [29]), it appears that the Frisch collar design offers excellent spectroscopic performance at the lowest cost, because complicated read-out electronics are unnecessary.

5. Conclusions

The uniformity of gamma ray response for a $4.7 \times 4.7 \times 9.5\,mm^3$ CdZnTe Frisch collar device has been investigated by probing the detector from the lateral side along the length and width with a collimated 662 keV gamma ray source. The results show uniform charge collection efficiency (CCE) over two-thirds of the device volume (Figs. 15 and 16), which was predicted with simple CCE simulations (Fig. 2). This uniform response was investigated experimentally and theoretically for a wide range of applied voltages. The reduced performance for irradiations in the near-anode region, where the Frisch collar effect is diminished, is mainly due to the low mobility-lifetime ($\mu\tau$) product of hole charge carriers. Note that the Frisch collar configuration is designed to negate the effects of severe hole trapping and low mobility. Hence, long CdZnTe Frisch collar device performance is dominated by electron motion, and therefore the performance will be limited almost entirely by the electron transport properties. As reported previously, a planar CdZnTe device shows a non-uniform response along device length [16]. Hence, planar CdZnTe detector designs are not well-suited for spectroscopic measurements of high energy gamma rays. Poor hole transport necessitates the use of advanced single carrier device designs. Among those, the Frisch collar design is one of the most inexpensive and robust.

Acknowledgments

This work was supported in part by DRTA Contract DTRA-01-03-C-0051, NSF Grant no. 0412208, and DOE Grant no. DE-FG07-04ID14599. The authors express their gratitude to Dr. Henry Chen and Dr. Salah Awadalla from Redlen Technologies for continued support and for providing the CdZnTe material investigated in this study.

References

[1] D.S. McGregor, R.A. Rojeski, US Patent no. 6,175,120, January 16, 2001.
[2] D.S. McGregor, US Patent no. 6,781,132, August 24, 2004.
[3] W.J. McNeil, D.S. McGregor, A.E. Bolotnikov, G.W. Wright, R.B. James, Appl. Phys. Lett. 84 (2004) 1988.
[4] A.E. Bolotnikov, G.S. Camarda, G.A. Carini, G.W. Wright, R.B. James, D.S. McGregor, W. McNeil, Proc. SPIE 5540 (2004) 33.
[5] A. Kargar, A.M. Jones, W.J. McNeil, M.J. Harrison, D.S. McGregor, Nucl. Instr. and Meth. A 558 (2) (2006) 497.
[6] H.H. Barrett, J.D. Eskin, H.B. Barber, Phys. Rev. Lett. 75 (1995) 156.
[7] P.N. Luke, IEEE Trans. Nucl. Sci. NS-42 (1995) 207.
[8] H.I. Malm, C. Canali, J.W. Mayer, M.A. Nicolet, K.R. Zanio, W. Akutagawa, Appl. Phys. Lett. 26 (1975) 344.
[9] D.S. McGregor, R.A. Rojeski, IEEE Trans. Nucl. Sci. NS-46 (3) (1999) 250.
[10] D.S. McGregor, Z. He, H.A. Seifert, R.A. Rojeski, D.K. Wehe, IEEE Trans. Nucl. Sci. NS-45 (1998) 443.
[11] D.S. McGregor, J. Nishanth, D. Wehe, Nucl. Instr. and Meth. A 457 (2001) 230.
[12] K. Parnham, J.B. Glick, Cs. Szeles, K.G. Lynn, J. Cryst. Growth 214/215 (2000) 1152.
[13] G. Montemont, M. Arques, L. Verger, J. Rustique, IEEE Trans. Nucl. Sci. NS-48 (2001) 278.
[14] L. Cirignano, H. Kim, K. Shah, M. Klugerman, P. Wong, M. Squillante, L. Li, Proc. SPIE 5198 (2004) 1.
[15] A.E. Bolotnikov, G.S. Camarda, G.A. Carini, G.W. Wright, L. Li, A. Burger, M. Groza, R.B. James, Phys. Stat. Sol. (c) (2005) 1495.
[16] M.J. Harrison, A. Kargar, D.S. McGregor, Nucl. Instr. and Meth. A 579 (2007) 134.
[17] V. Radeka, Ann. Rev. Nucl. Part. Sci. 38 (1988) 217.
[18] W. Shockley, J. Appl. Phys. 9 (1938) 635.
[19] S. Ramo, Proc. I.R.E. 27 (1939) 584.
[20] G. Cavalleri, G. Fabri, E. Gatti, V. Svelto, Nucl. Instr. and Meth. 21 (1963) 177.
[21] J.B. Gunn, Solid State Electron. 7 (1964) 739.
[22] P.A. Tove, K. Falk, Nucl. Instr. and Meth. 29 (1964) 66.
[23] M. Martini, G. Ottaviani, Nucl. Instr. and Meth. 67 (1969) 177.
[24] G. Cavalleri, E. Gatti, G. Fabri, V. Svelto, Nucl. Instr. and Meth. 92 (1971) 137.
[25] A. Kargar, A.C. Brooks, M.J. Harrison, H. Chen, S. Awadalla, G. Bindley, B. Redden, D.S. McGregor, Proc. SPIE 7449 (2009) 744908-01-744908-13.
[26] T.H. Prettyman, M.K. Smith, S.E. Soldner, Proc. SPIE 3768 (1999) 339.
[27] A. Kargar, A.C. Brooks, M.J. Harrison, R.B. Lowell, R.C. Keyes, H. Chen, G. Bindley, D.S. McGregor, IEEE Trans. Nucl. Sci. NS-56 (2009) 824.
[28] G. De Geronimo, E. Vernon, K. Ackley, A. Dragone, J. Fried, P. O'Connor, Z. He, C. Herman, F. Zhang, IEEE Trans. Nucl. Sci. NS-55 (2008) 1593.
[29] R. Gonzaleza, J.M. Pereza, Z. He, Nucl. Instr. and Meth. A 531 (2004) 544.